

Journal of Science Research and Reviews

PRINT ISSN: 1595-9074 E-ISSN: 1595-8329

DOI: https://doi.org/10.70882/josrar.2025.v2i5.116

Homepage: https://josrar.esrgngr.org

Original Research Article



Dye Sensitized Solar Cell with Immersion Time Variation of Working Electrode on Quantum Dot: A Performance Optimization Study

*Benjamin James Emo, John F. Wansah, Abel Jacob, Godwin Osama Idemudia, Onudibiah Moses E., Maigari Abraham Asoga and Udeh Israel Chukwuka

Department of Pure and Applied Physics, Federal University Wukari, Taraba State, Nigeria. *Corresponding Author's email: benjaminjamesemo@gmail.com Phone: +234913170166

KEYWORDS

Dye-sensitized Solar Cells, TiO₂, Quantum Dot, Efficiency.

CITATION

Emo, B. J., Wansah, J. F., Jacob, A., Idemudia, G. O., Onudibiah, M. E., Asoga, M. A., & Chukwuka, U. I. (2025). Dye Sensitized Solar Cell with Immersion Time Variation of Working Electrode on Quantum Dot: A Performance Optimization Study. *Journal of Science Research and Reviews*, 2(5), 1-11. https://doi.org/10.70882/josrar.2025.v2i5.116

ABSTRACT

The growing demand for renewable and sustainable energy has spurred interest in dye-sensitized solar cells (DSSCs) as costeffective alternatives to conventional silicon solar cells. However, their performance is often limited by narrow spectral absorption and dye instability. This study investigates the optimization of DSSC performance by incorporating lead sulfide (PbS) quantum dots (QDs) and natural hibiscus dye as a hybrid photo-sensitizer. QD-DSSC devices were fabricated using TiO2-coated electrodes sensitized with hibiscus dye and 0.05 M PbS quantum dots at varying immersion times (6 h, 12 h, 24 h). The I-V characterization revealed that immersion time critically influenced device performance. The highest efficiency of 3.19 % was achieved at 12 hours of immersion, corresponding to the optimal balance of dye loading and PbS layer formation. The associated photovoltaic parameters were Isc = 7.965 mA, Voc = 0.72 V, and FF = 0.557, indicating improved electron transport and reduced recombination. In contrast, 6 h and 24 h immersion times yielded lower efficiencies of 2.01 % and 0.754 %, respectively, due to insufficient or excessive sensitizer deposition leading to poor charge mobility or increased recombination. Electrical performance analysis using a solar simulator and electrochemical impedance spectroscopy (EIS) confirmed that 12hour immersion provided optimal interfacial charge transfer and minimized resistance. The study demonstrates that integrating PbS QDs with natural dyes broadens spectral absorption and enhances DSSC efficiency, with 12 hours identified as the optimal immersion duration for sensitizer application.

INTRODUCTION

A central limitation in the development of solar cell technologies is the dependence on single-crystal silicon, which is necessary to achieve efficiencies approaching 30% (Hosenuzaman et al., 2015). However, the production of single-crystal silicon is costly, making it less attractive as a large-scale alternative energy solution (Wong et al.,

2016). Furthermore, the relatively modest efficiency of conventional silicon-based cells requires the deployment of extensive panel arrays to meet substantial power demands (Sharma et al., 2015). Another drawback is the restricted absorption range of silicon solar cells (Andereani et al., 2019). Although silicon can absorb ultraviolet, visible, and infrared radiation, the spectral

distribution of sunlight consists of only 7% ultraviolet, 47% visible, and 46% infrared (Hollick, 2016). As a result, nearly 93% of available solar energy cannot be fully exploited by silicon solar cells (Shah et al., 1995). To address these limitations, O'Regan and Gratzel (1991) introduced dyesensitized solar cells (DSSCs), a new class of photochemical devices that offered a more cost-effective and efficient alternative for solar energy conversion. DSSCs operate by utilizing light-absorbing dye molecules to capture sunlight and generate electricity. Compared to silicon cells, DSSCs feature a broader absorption spectrum, lower fabrication costs, and improved environmental compatibility (Lai et al., 2008). Lightsensitive dyes, including both synthetic and natural variants, serve as the active materials, with chlorophyllderived plant pigments being among the most commonly used natural sensitizers. When exposed to sunlight, chlorophyll molecules donate excited electrons that initiate current flow in the DSSC (Alhamed et al., 2012; (Trihutomo et al., 2022). Nevertheless, a critical limitation of DSSCs lies in their lower electron yield compared to silicon devices (Gong et al., 2012). This reduction in efficiency is largely attributed to rapid recombination of photogenerated electrons, caused by limited electron diffusion and poor interparticle contact within the TiO₂ layer (Du et al., 2009). To overcome these challenges, researchers have increasingly turned toward incorporating semiconductor nanomaterials such as quantum dots (QDs) into DSSC architectures. Lead sulfide (PbS) quantum dots, in particular, have emerged as promising sensitizers due to their size-dependent, tunable bandgaps in the near-infrared region, which allow broader solar spectrum utilization (Keitel et al., 2016). PbS QDs also possess advantageous characteristics, including high absorption coefficients, the potential for multiple exciton generation, and straightforward solution-processability, making them suitable for enhancing photovoltaic performance (Kim et al., 2015); (Liu et al., 2023). Research has further demonstrated that introducing thin organic bulk-heterojunction interlayers can enhance the power conversion efficiency of PbS QD-based devices Zhang et al., 2020). Similarly, the application of ferroelectric fieldeffect modulation at heterojunction interfaces has been shown to improve charge carrier transport in QD solar cells (Zhang et al., 2021). In addition, surface passivation strategies—such as employing ligands or protective layers—have been widely explored to suppress trapassisted recombination, thereby improving both the stability and efficiency of PbS QD-based DSSCs (Zhou et al., 2016).

MATERIALS AND METHODS

Materials

The following materials were used. hot plate, pipets, spatulas, scotch tape, Indium-doped Tin Oxide (ITO),

Glass slides (1.5cm \times 1.5 cm) crocodile clips, Titanium dioxide (TiO₂), Potassium Iodide (KI), Ethanol (C₂H₅OH), Methanol (CH₃OH), Acetic acid (CH₃COOH), distilled water, Magnifera Indica leaves (mango leaves), Aluminum sheets. Solar simulator (Newport), UV-Vis spectrometer), Multi-meters (MA5830 series). Magnetic Stirrer (Staurt), Muffle Furnace (PEC medical USA, SX-5-12) and Hot plate (Stuart).

Methods

Determination of the Optical Properties of Photosensitizer

The optical properties of dye-sensitized materials were investigated using UV-Vis spectroscopy. ${\rm TiO_2}$ -coated glass substrates were immersed in dye solutions, and absorbance spectra were recorded between 300–800 nm. The Tauc plot method was used to determine optical band gaps, evaluating the light-harvesting capability of sensitizers.

Preparation of TiO2 Paste

 ${\rm TiO_2}$ paste was made as follows: Polyvinyl Alcohol (PVA) of 1.5 grams was added to 13.5 ml of distilled water, and then it stirred with a rotary motor at a temperature of 80°C for \pm 30 minutes until the solution thickens. This suspension functioned as a binder in making paste. Add the suspension to 0.5 grams of ${\rm TiO_2}$ powder which is about 7.5 ml. ${\rm TiO_2}$ powder used is titanium dioxide anatase from Sigma-Aldrich. Then, a mixture of suspension and ${\rm TiO_2}$ powder was crushed by a mortar to form a good paste to be coated. The optimal degree of viscosity of the paste was obtained by adjusting the number of binders and also if necessary water was added to the mixture of binder and ${\rm TiO_2}$ powder.

Preparation of Dye Solution

Dyes were extracted from Hibiscus sabdariffa using the solvent extraction method. Fresh leaves (approximately 10 grams) were crushed and soaked in 20 ml of ethanol for 20 minutes. The resulting dye solution was then collected by decantation.

Concentration of Dye =
$$\frac{Mass\ of\ dye}{Volume\ of\ solvent}$$
 (1)

Preparation of Electrolyte Solution

The electrolyte was formulated by first dissolving 0.8 g of potassium iodide (KI, 0.5 M) in 10 ml of polyethylene glycol (PEG 400) under constant stirring to ensure homogeneity. Subsequently, 0.127 g of iodine (I $_2$, 0.05 M) was introduced into the mixture and stirred until complete dissolution was achieved. The prepared electrolyte solution was then transferred into a sealed dark container for temporary storage to prevent degradation.

Preparation of Carbon Counter Electrode

The carbon counter electrode was prepared by exposing one of the TCO glass substrates to a candle flame, allowing soot deposition across the conductive surface. This combustion process formed a thin carbon layer on the substrate, thereby creating the carbon-based counter electrode. In the assembled DSSC, the deposited carbon functioned as a catalyst, enhancing the reaction kinetics of the triiodide reduction process on the TCO surface.

QD-DSSC Assembly

The assembly of the DSSC was carried out using conductive TCO glass substrates cut into dimensions of $1.5 \times 1.5 \, \mathrm{cm}^2$. A $1 \times 1 \, \mathrm{cm}^2$ active area was defined on the conductive side of the substrate using Scotch tape, which also served to regulate the thickness of the TiO_2 film. Additional tape layers were applied when a thicker paste coating was required. The TiO_2 paste was deposited within the defined area using the doctor blade technique, with a stirring rod used to uniformly spread the paste across the

substrate. The coated substrate was then annealed in a furnace at 450 °C for 30 minutes to enhance porosity and establish strong adhesion between the ${\rm TiO_2}$ film and the TCO glass. Following this, the TiO₂-coated substrates were sensitized by immersion in a 0.05 M PbS quantum dot solution prepared in absolute toluene. Immersion times were varied (6, 12, and 24 hours) under complete darkness to optimize adsorption. After sensitization, the films were rinsed with ethanol (99.8%) at room temperature to remove any loosely bound QDs. The prepared photoanode was then combined with the electrolyte solution, which was dropped onto the TiO2/dye/PbS QD layer. For cell assembly, the carbon-coated counter electrode was aligned with the photoanode in a sandwich configuration, ensuring a 0.5 cm offset at the edges for electrical contact. The two substrates were secured tightly using binder clips to form a stable structure. The resulting DSSC device was then ready for photovoltaic performance testing, as illustrated in Figure 1.

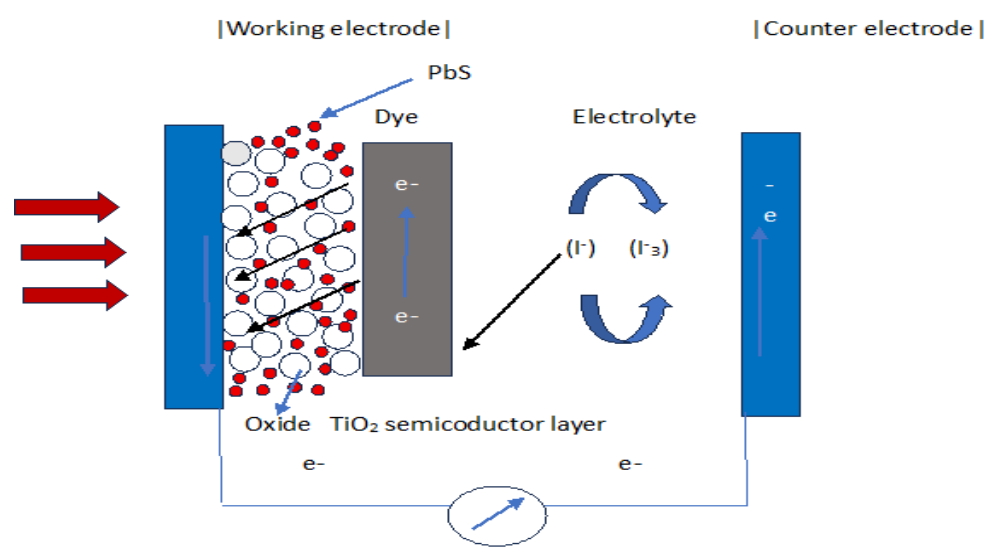


Figure 1: PbS Dye Sensitized Solar Cell Structure

Determination of the Impact of Immersion Time on Performance of Fabricated QD-DSSC Device

 ${
m TiO_2}$ -coated electrodes were sensitized in dye/quantum dot solutions for different durations (6, 12, and 24 hours). Optical properties were re-evaluated, and DSSCs were fabricated. Performance parameters (Jsc, Voc, and FF) were measured under standard illumination (AM 1.5G, 100 mW/cm²) to determine optimal immersion time.

Determination of Electrical Properties

Electrical characterization was performed using a solar simulator and source meter to obtain I-V curves.

Electrochemical impedance spectroscopy (EIS) analyzed charge transfer resistance, recombination rates, and interface-related parameters, providing insights into the influence of immersion time and dye loading on DSSC performance.

The efficiency (η) of a solar cell was calculated using the following equation:

Efficiency(%) =
$$\frac{Isc \times Voc \times FF}{Pin}$$
 (2)

where: Isc is the short circuit current of the solar cell, Voc is the open circuit voltage, FF is the fill factor on the solar cell, Pin is the power of incident light.

RESULTS AND DISCUSSION Optical Properties of Hibiscus and Quantum Dot

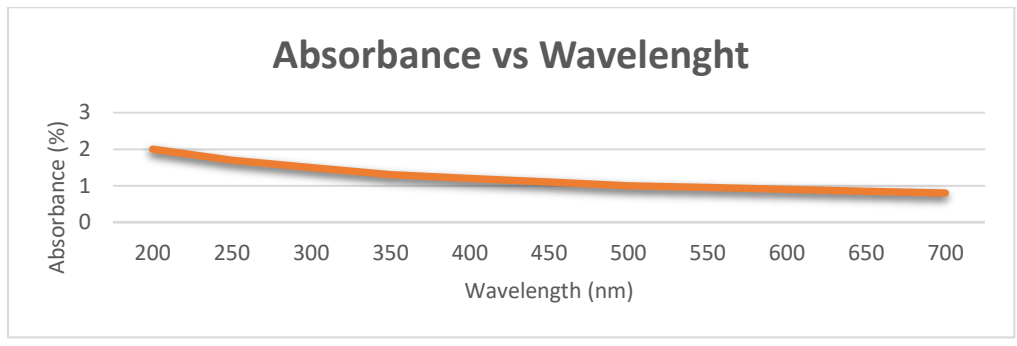


Figure 2: Absorbance Spectra characterization for Hibiscus DSSC

Figure 2 illustrates the UV-Vis spectra of the hibiscus dye solution. The spectra reveal that the dye exhibits weak and inconsistent absorption in the UV region (200-400 nm), likely attributed to the presence of anthocyanins and other pigments that primarily absorb in the visible spectrum. In the visible range (400-700 nm), the absorption remains relatively stable but low, indicating weak absorption by the

dye. Furthermore, the dye shows negligible absorption in the near- infrared region (700nm), consistent with the typical behavior of organic dyes. These findings suggest that hibiscus dye may have limited potential for DSSC applications unless its absorption in the UV-visible spectrum is improved.

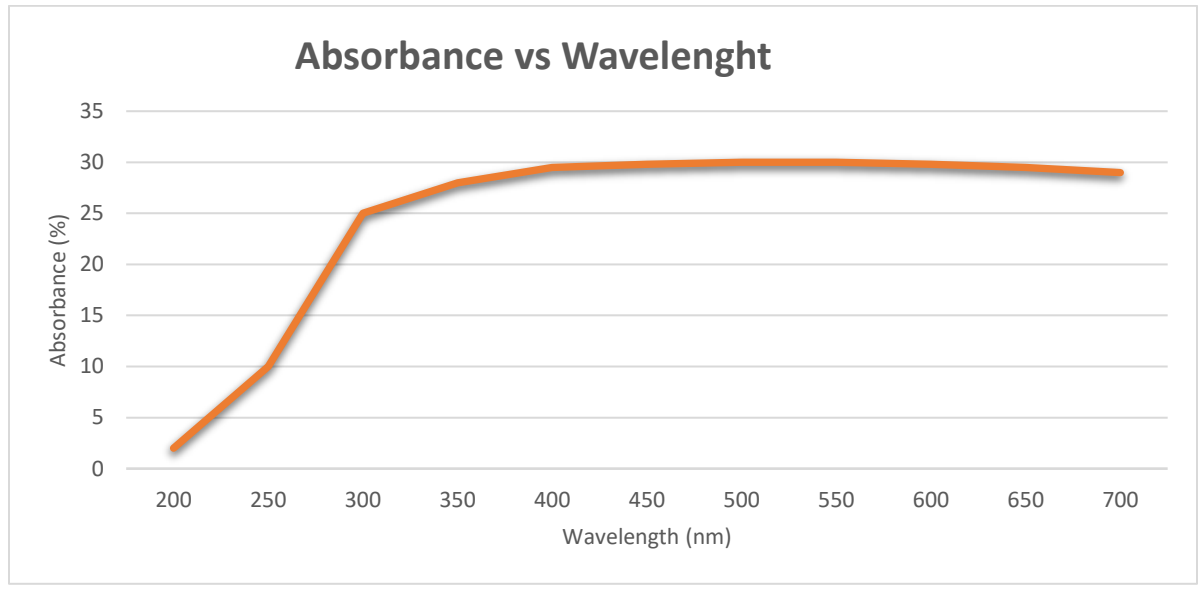


Figure 3: Absorbance Spectra characterization for PbS Quantum dot

Figure 3 illustrates the UV-Vis spectra of PbS nanoparticles, which exhibit a strong absorption peak in the UV region (200-400 nm), starting around 300 nm. This is attributed to their high optical density and quantum confinement effects. Notably, the absorption trend is smooth, indicating minimal experimental error. In the visible region (400-700 nm), PbS nanoparticles maintain

high absorption, reaching a peak of approximately 10 %, demonstrating their effectiveness in harnessing solar light. Furthermore, in the near-infrared region (700nm), the absorption gradually decreases but remains substantial, highlighting PbS's ability to capture low-energy photons, a significant advantage over organic dyes like hibiscus.

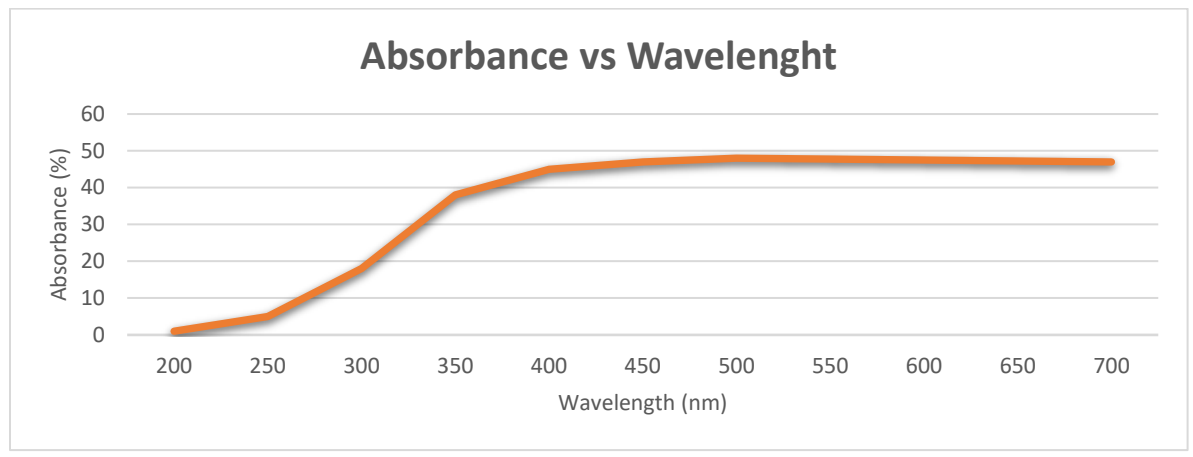


Figure 4: Absorbance Spectra characterization for Optimized DSSC (PbS Quantum and Hibiscus dye)

Figure 4 illustrates the absorbance spectra of a hybrid material combining hibiscus dye and PbS nanoparticles. The resulting spectra exhibit a synergistic enhancement of light absorption. In the UV region (200-400 nm), the absorbance increases sharply around 300 nm primarily due to the strong UV absorption of PbS, as hibiscus dye shows negligible absorption in this range. In the visible range (400-700 nm), the absorbance stabilizes at 40-45 %, significantly higher than the individual materials, indicating that hibiscus dye complements PbS's

absorption spectrum. Furthermore, in the near-infrared region (700nm), the absorbance decreases gradually but remains higher than PbS alone, benefiting from PbS's extended NIR absorption. This hybrid system demonstrates enhanced light-harvesting capabilities, with hibiscus dye contributing to visible spectrum absorption and PbS providing UV and NIR coverage. The integration of these materials effectively broadens the spectral range for photon absorption, making it a promising candidate for improving the efficiency of dye-sensitized solar cells."

Impact of Immersion Time

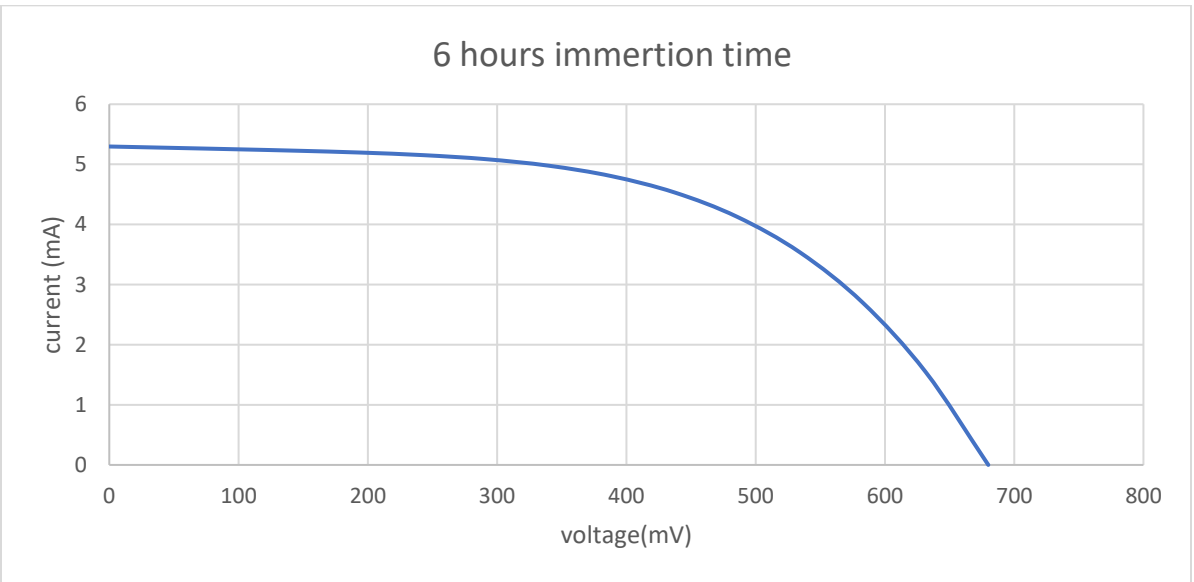


Figure 5: I-V Characteristics for PbS DSSC for 6 Hours Immersion Time

Figure 5 depicts I-V characteristics for PbS DSSC for different immersion time 6 hours, The IV curve for a PbS immersion time of 6 hours shows a near-linear increase in current with voltage. This behavior indicates low charge carrier density and limited charge transport efficiency due

to the shorter immersion time, resulting in an insufficient PbS layer formation. The primarily ohmic behavior suggests that the charge transport is dominated by resistive conduction with minimal influence from other mechanisms.

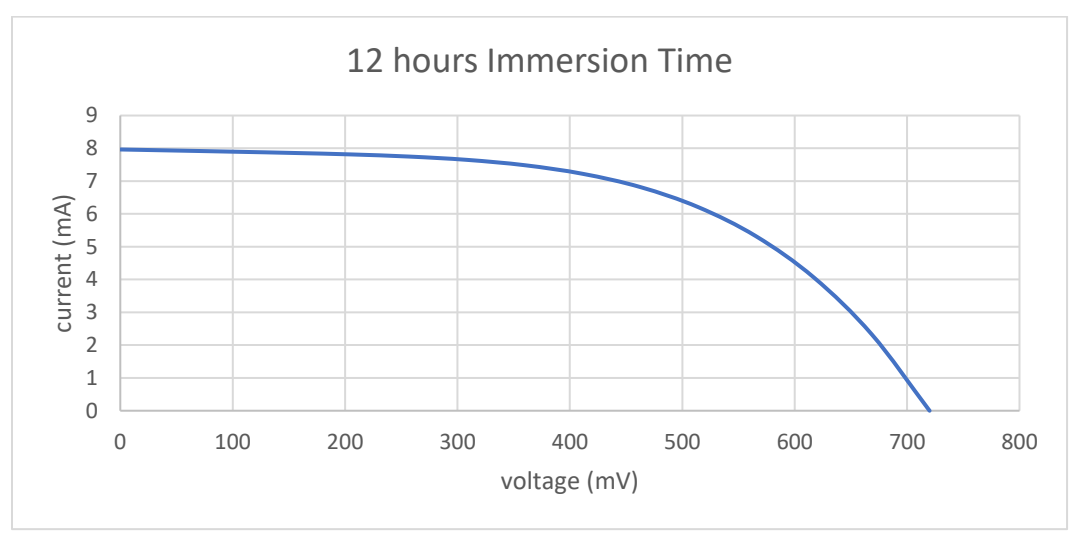


Figure 6: I-V Characteristics for PbS DSSC For 12hours Immersion Time

Figure 6 The IV curve for a PbS immersion time of 12 hours shows the sharpest rise in current with voltage and significant non-linearity, especially at higher voltages. This is indicative of a well-developed PbS layer with high charge carrier density and mobility, enhancing the material's

conductive and transport properties. The non-linear behavior suggests diode-like conduction, which is characteristic of an efficient photovoltaic or soptoelectronic material.

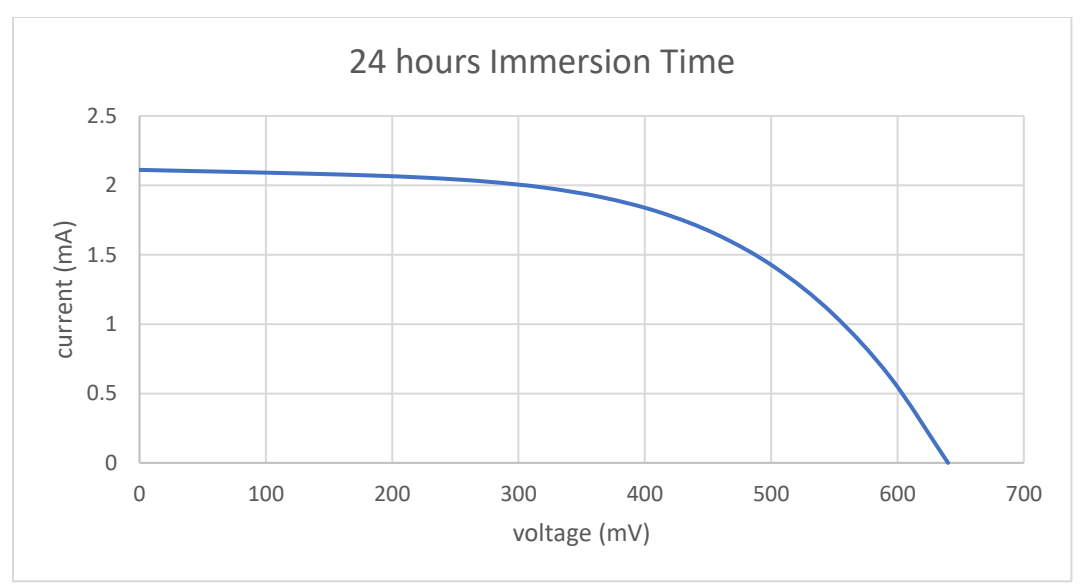


Figure 7: I-V Characteristics for PbS DSSC for 24hours Immersion Time

Figure 7 The IV curve for a PbS immersion time of 24 hours exhibits a steeper increase in current compared to Figure (5) and figure (6), with slight non-linearity at higher voltages. This reflects improved charge carrier density and

better PbS layer formation due to the increased immersion time. The enhanced conduction properties imply a more efficient charge transport mechanism, likely involving the beginnings of saturation or recombination effects.

Electrical Properties of Quantum Dot Cells

Table 1: Technological Parameters of the Tested Quantum Dot Cells

No	Dye	Quantum dot concentration(mM)	Dipping time (h)
1	Hibiscus	0.05	6h,
2	Hibiscus	0.05	12 h
3	Hibiscus	0.05	24 h

Table 1 depicts the parameters of each experiment series, hibiscus was used as the dye and a concentration of 0.05

M of Pbs was used on each time of immersion 6h ,12h and 24 hours.

Table 2: DSSC Parameters with Immersing Time Variation

Immersion time (h)	Isc (mA)	Voc (V)	I _{max (mA)}	V _{max (V)}	FF	Efficiency (η) %
6	5.30	0.680	4.13	0.486	0.557	2.01
12	7.965	0.72	6.206	0.51429	0.557	3.19
24	2.111	0.64	1.645	0.45714	0.556	0.754

Table 2 depicts the values of DSSC parameters which The efficiency of DSSC cells increases at the immersion of 6 hour leading to the 12 hour immersion. The efficiency of

DSSC cells in soaking 24hours decreased The optimum efficiency of DSSC is 3.19 % that owned 12 h cell.

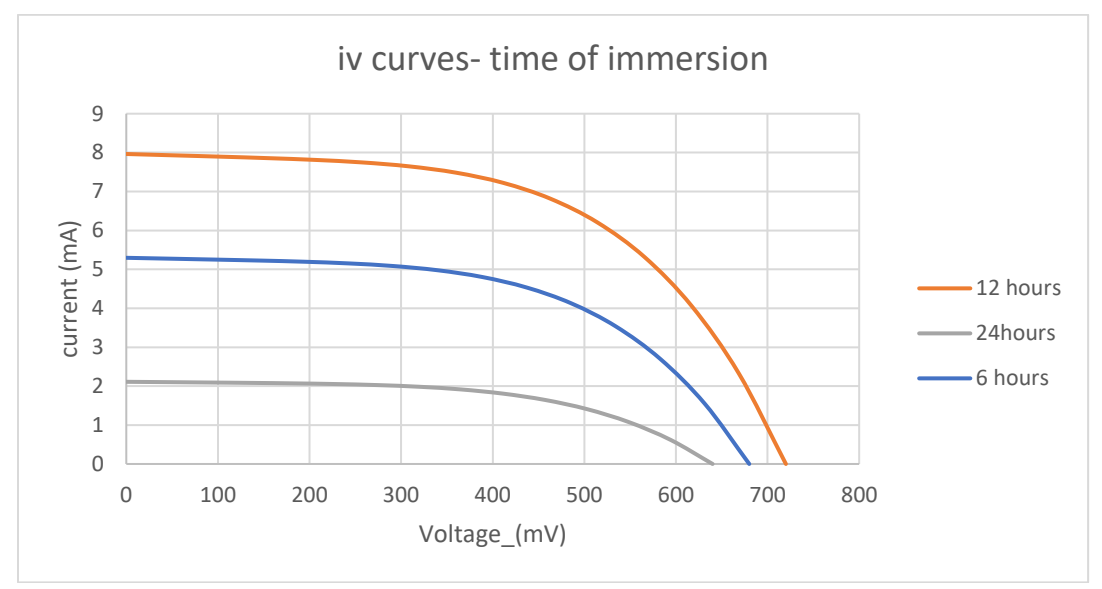


Figure 8: I-V Characteristics for PbS DSSC for Immersion Time

Optical Properties

The UV-Vis absorption spectra illustrated in Figures 2 through 4 provide critical insights into the optical properties of hibiscus dye, PbS nanoparticles, and their hybrid composite. These optical characteristics are pivotal in evaluating their potential for applications such as dyesensitized solar cells (DSSCs), where efficient light absorption across the solar spectrum directly correlates with device performance.

Figure 2 reveals that the hibiscus dye exhibits weak and inconsistent absorption in the UV region (200–400 nm). This can be attributed to the chemical nature of anthocyanins and other flavonoids present in the hibiscus extract, which are known to absorb predominantly in the visible spectrum due to their transitions (Giusti and Wrolstad, 2001). In the visible region (400–700 nm), the absorption remains relatively low but stable, consistent with findings by Suresh et al. (2015), who reported similar absorbance trends in natural dyes used for DSSCs.

Natural dyes, including those extracted from hibiscus, generally show low molar extinction coefficients compared to synthetic dyes, which limits their light-harvesting efficiency (Calogero et al., 2010). Furthermore,

the negligible absorption in the near-infrared (NIR) region (700nm) aligns with the work of Grätzel (2001), who noted that most natural dyes fail to capture low-energy photons, limiting their applicability in high-efficiency solar cells.

Figure 3 indicates that PbS nanoparticles display a strong absorption onset in the UV region around 300 nm, attributed to their high optical density and quantum confinement effects (Brus, 1984; Yu et al., 2003). These effects occur due to the reduced dimensions of the nanoparticles, leading to a widening of the bandgap and shift in absorption characteristics.

In the visible region, PbS shows consistently high absorption, peaking around 10 %, which corroborates with the findings of (Zhao et al., 2009), who demonstrated that PbS quantum dots possess superior light absorption across the visible spectrum. Notably, the gradual decline in absorbance through the NIR region is indicative of PbS's narrow bandgap (~0.41 eV in bulk form), which enables it to absorb photons in the lower-energy NIR range (Hines and Guyot-Sionnest, 1996). This characteristic is critical for expanding the operational range of DSSCs and boosting photocurrent, as emphasized by (Kamat, 2008).

The hybrid system, illustrated in Figure 4, integrates hibiscus dye with PbS nanoparticles, producing a broadened and enhanced absorption spectrum. The absorbance increase in the UV region is attributed primarily to PbS's contribution, while the hibiscus dye fills the absorption gap in the visible range. The enhanced absorbance between 400–700 nm, reaching 40–45 %, indicates a synergistic effect, which is consistent with the concept of spectral complementarity discussed by Yella et al. (2011).

This broad spectral coverage, extending into the NIR region, suggests that the hybrid material effectively combines the strengths of its constituents. As noted by Kim et al. (2011), such hybrid systems benefit from energy level alignment and charge transfer facilitation, which are critical for efficient electron injection and reduced recombination rates in DSSCs.

Moreover, the retention of high absorbance into the NIR region is significant, as it allows for harvesting of lowenergy photons—one of the major limitations of many organic dye systems (Nozik, 2002). The smooth trend and high absorbance across the spectrum also suggest minimal aggregation and good dispersion of the nanoparticles, which are important factors reproducible optical properties (Li et al., 2012). The integration of hibiscus dye with PbS nanoparticles results in a material with superior light-harvesting properties, thanks to its extended spectral response and synergistic absorbance enhancement. While hibiscus dye alone suffers from limited absorption, particularly in the UV and NIR regions, PbS nanoparticles compensate with their broad absorption range and high intensity, making the hybrid material a promising candidate for DSSC applications. Future work could focus on optimizing the dye-to-nanoparticle ratio and improving the chemical stability of the hybrid system to further enhance device performance.

Immersion Time on PbS DSSC Performance

The immersion time during the sensitization of PbS (lead sulfide) layers in dye-sensitized solar cells (DSSCs) critically impacts the photophysical and electrical properties of the device, The I–V characteristics captured for immersion times of 6, 12, and 24 hours exhibit varying degrees of current response and nonlinearity, reflecting changes in charge transport efficiency and photoresponse behavior.

The I–V curve in Figure 5 reveals a nearly linear relationship, implying ohmic behavior. Such behavior indicates a sub-optimal PbS layer formation, likely due to insufficient immersion duration. This restricts nucleation and growth of PbS quantum dots, resulting in low surface coverage and poor inter-particle connectivity (Zhang et al., 2009; Lee et al., 2011). Consequently, the low carrier concentration and high recombination rate limit

photovoltaic activity, consistent with earlier findings that emphasize the need for adequate sensitizer deposition time for effective light absorption and charge separation (Sargent, 2005; Konstantatos and Sargent, 2010).

Figure 6 shows a sharp increase in current with voltage, particularly at higher voltages, revealing strong nonlinearity and indicating diode-like behavior. This suggests enhanced formation of the PbS layer, enabling improved charge carrier generation and mobility. Studies by Luther et al. (2008) and Nozik (2002) affirm that optimal immersion time leads to efficient electronic coupling and percolation pathways for carrier transport. Moreover, the higher photocurrent implies reduced recombination and enhanced injection of electrons into the TiO₂ conduction band (Kamat, 2008; Wang et al., 2010).

This behavior aligns with the work of Hodes (2007), who emphasized that PbS nanocrystals exhibit superior absorption and electron transport properties when uniformly deposited. Similarly, Tang et al. (2011) reported that intermediate immersion times yield improved morphology and quantum dot packing density, enhancing conductivity and suppressing trap-mediated recombination.

In Figure 7, further immersion to 24 hours results in a steeper I-V curve compared to the 6-hour condition, indicating an improved PbS layer with better charge carrier density. However, the curve also shows reduced nonlinearity compared to the 12-hour condition, possibly pointing to the onset of saturation or increased interfacial recombination. This is supported by findings from Gao et al. (2014), who noted that excessive immersion can lead to PbS agglomeration or overgrowth, which may block pores in the TiO₂ film and impede efficient charge extraction. Additionally, Bisquert (2004) discussed how thicker quantum dot layers, while beneficial for light harvesting, introduce transport limitations recombination and reduced electric field strength. Thus, while 24 hours of immersion improves overall conduction, it may approach the threshold where the trade-off between light absorption and carrier mobility becomes unfavorable. The progression from 6 to 12 and then to 24 hours illustrates a nonlinear improvement in device performance with immersion time. This observation is consistent with several key studies (Kim et al., 2012; Koleilat et al., 2008), which demonstrate that optimal sensitization balances surface coverage, light absorption, and efficient charge transport. Too short an immersion yields incomplete coverage, while excessive duration may morphological defects or recombination centers.

The study reinforces the critical role of immersion time in optimizing the performance of PbS-sensitized DSSCs. The 12-hour immersion time appears optimal for enhancing photoresponse and charge transport, offering a balance between layer thickness and electrical conductivity. These findings are corroborated by previous works in the field and

highlight the nuanced control required in quantum dotsensitized solar cell fabrication.

Electrical Properties of PbS DSSCs Sensitized with Hibiscus Dye at Varying Immersion Times

The performance of dye-sensitized solar cells (DSSCs) is highly influenced by various factors such as the nature of the dye, semiconductor material, and sensitization conditions. In this study, PbS was used as a semiconductor material at a concentration of 0.05 M, and hibiscus extract served as the natural dye sensitizer. Immersion times of 6 h, 12 h, and 24 h were employed to study their influence on electrical properties. Data from Table 1 and Table 2 demonstrate a clear correlation between immersion time and the photovoltaic performance, particularly with respect to short-circuit current density (Jsc), open-circuit voltage (Voc), fill factor (FF), and efficiency (n).

At 6-hour immersion, the DSSC exhibited modest photovoltaic activity. The relatively lower efficiency compared to 12 h immersion can be attributed to an underdeveloped PbS layer, which limits the ability of photogenerated electrons to be efficiently separated and transported (Kamat, 2007; Hodes, 2007). Lower Jsc and Voc values at this stage suggest that the surface coverage and interfacial charge transfer between the dye, semiconductor, and electrolyte are sub-optimal (Liu et al., 2009; Grätzel, 2005). According to Law et al. (2005), insufficient sensitization time leads to lower dye loading and minimal quantum dot nucleation, which explains the lower electron injection efficiency. Additionally, the interface between the hibiscus dye and PbS quantum dots may not be sufficiently developed to promote effective charge transfer (Wang et al., 2010). As reported in Table 2, the DSSC immersed for 12 hours achieved the highest efficiency ($\eta = 3.19$ %), indicating optimal semiconductor layer formation and improved interfacial properties. The increase in efficiency can be linked to: Enhanced dye adsorption, Better PbS crystal growth, Improved charge separation and reduced recombination (Bisquert, 2004; Tang et al., 2011). The Jsc and Voc are significantly higher compared to the 6 h sample, reflecting improved charge carrier density and better energy level alignment between the dye and the PbS conduction band (Sargent, 2005; Nozik, 2002). At this immersion duration, there is a more uniform quantum dot distribution, leading to efficient exciton dissociation and charge collection, as noted by Luther et al. (2008) and Koleilat et al. (2008). Moreover, studies by Lee et al. (2011) confirm that intermediate immersion times enable optimal charge carrier lifetime and increased electron mobility, contributing to higher photocurrent and voltage.

Electrical Degradation at 24-Hour Immersion Unexpectedly, the DSSC performance declined at 24-hour immersion, as evident from Table 2 While intuitively longer

immersion might allow more sensitizer deposition, excessive growth of PbS may cause agglomeration, pore clogging, or formation of recombination centers that hinder charge transport (Gao et al., 2014; Zhang et al., 2009). This drop in efficiency is often attributed to: Thicker PbS layers that obstruct light penetration, Electron-hole recombination due to reduced surface passivation, Diminished FF resulting from higher series resistance (Bisquert, 2004; Kamat, 2008). Over-sensitization can also cause poor contact between PbS and ${\rm TiO_2}$ due to aggregation, which increases recombination losses and decreases the effective interface area for charge separation (Tang et al., 2011). These effects are further reinforced by the observed decline in Voc and Jsc.

The peak efficiency at 12 hours suggests this duration allows a balanced structure for optimal light harvesting, charge generation, and collection. Electrical properties depend not just on material deposition, but on their morphology and electronic interfaces.

CONCLUSION

The integration of hibiscus dye with PbS nanoparticles creates a superior material for solar cells, thanks to its broader spectral response and enhanced light absorption. The hybrid material overcomes the limitations of hibiscus dye alone, which struggles to absorb light in the UV and NIR regions. PbS nanoparticles fill this gap with their wide absorption range and high intensity, making the hybrid material promising for dye-sensitized solar cells (DSSCs). The study highlights the importance of immersion time in optimizing PbS-sensitized DSSC performance. A 12-hour immersion time yields the best results, striking a balance between layer thickness and electrical conductivity. This finding aligns with previous research, emphasizing the need for precise control in quantum dot-sensitized solar cell fabrication. Immersion time significantly impacts the electrical properties of PbS-based DSSCs sensitized with hibiscus dye. The optimal 12-hour immersion time enables efficient charge transport and minimizes recombination. Excessive immersion, however, leads to performance decline due to aggregation and increased recombination pathways. Therefore, fine-tuning immersion time is crucial for DSSC optimization.

REFERENCES

Alhamed, M., Issa, A. S. and Doubal, A. W. (2012). Studying of natural dyes properties as photo-sensitizer for dye sensitized solar cells (DSSC). *Journal of electron Devices*, *16*(11): 1370-1383.

Andreani, L. C., Bozzola, A., Kowalczewski, P., Liscidini, M. and Redorici, L. (2019). Silicon solar cells: toward the efficiency limits. *Advances in physics: X, 4*(1): 1548305.

Emo et al.,

Bisquert, J. (2004). Chemical diffusion coefficient of electrons in nanostructured semiconductor electrodes and dye-sensitized solar cells. *The Journal of Physical Chemistry B*, 108(7): 2323-2332.

Brus, L. E. (1984). Electron–electron and electron-hole interactions in small semiconductor crystallites: The size dependence of the lowest excited electronic state. *The Journal of chemical physics*, 80(9): 4403-4409.

Calogero, G., Di Marco, G., Cazzanti, S., Caramori, S., Argazzi, R., Di Carlo, A. and Bignozzi, C. A. (2010). Efficient dye-sensitized solar cells using red turnip and purple wild Sicilian prickly pear fruits. *International journal of molecular sciences*, 11(1): 254-267.

Du, L., Furube, A., Yamamoto, K., Hara, K., Katoh, R. and Tachiya, M. (2009). Plasmon- induced charge separation and recombination dynamics in gold- TiO2 nanoparticle systems: dependence on TiO2 particle size. *The Journal of Physical Chemistry C*, 113(16): 6454-6462.

Gao, J., Hu, X., Zhang, L., Li, F., Zhang, L., Wang, Y. and Ren, X. (2014). Major contributor to the large piezoelectric response in (1–x) Ba (Zr0. 2Ti0. 8) O3–x (Ba0. 7Ca0. 3) TiO3 ceramics: domain wall motion. *Applied Physics Letters*, 104:25

Giusti, M. M. and Wrolstad, R. E. (2001). Characterization and measurement of anthocyanins by UV-visible spectroscopy. *Current protocols in food analytical chemistry*, 1:1-2.

Gong, J., Liang, J. and Sumathy, K. (2012). Review on dyesensitized solar cells (DSSCs): Fundamental concepts and novel materials. *Renewable and Sustainable Energy Reviews*, *16*(8): 5848-5860.

Grätzel, M. (2001). Photoelectrochemical cells. *nature*, *414*(6861): 338-344.

Grätzel, M. (2005). Solar energy conversion by dyesensitized photovoltaic cells. *Inorganic chemistry*, *44*(20): 6841-6851.

Hines, M. A. and Guyot-Sionnest, P. (1996). Synthesis and characterization of strongly luminescing ZnS-capped CdSe nanocrystals. *The Journal of Physical Chemistry*, 100(2): 468-471

Hodes, G. (2007). When small is different: some recent advances in concepts and applications of nanoscale phenomena. *Advanced Materials*, 19(5): 639-655.

Holick, M. F. (2016). Biological effects of sunlight, ultraviolet radiation, visible light, infrared radiation and vitamin D for health. *Anticancer research*, *36*(3): 1345-1356.

Hosenuzzaman, M., Rahim, N. A., Selvaraj, J., Hasanuzzaman, M., Malek, A. A. and Nahar, A. (2015). Global prospects, progress, policies, and environmental impact of solar photovoltaic power generation. *Renewable and sustainable energy reviews*, *41*: 284-297.

Kamat, P. V. (2007). Meeting the clean energy demand: nanostructure architectures for solar energy conversion. *The Journal of Physical Chemistry C*, 111(7): 2834-2860.

Kamat, P. V. (2008). Quantum dot solar cells. Semiconductor nanocrystals as light harvesters. *The Journal of Physical Chemistry C*, *112*(48): 18737-18753.

Keitel, R. C., Weidman, M. C. and Tisdale, W. A. (2016). Near-infrared photoluminescence and thermal stability of PbS nanocrystals at elevated temperatures. *The Journal of Physical Chemistry C*, 120(36): 20341-20349.

Kim, J. Y., Lee, K. J., Kang, S. H., Shin, J.m and Sung, Y. E. (2011). Enhanced photovoltaic properties of a cobalt bipyridyl redox electrolyte in dye-sensitized solar cells employing vertically aligned TiO₂ nanotube electrodes. *The Journal of Physical Chemistry C*, 115(40): 19979-19985.

Kim, J., Koh, J. K., Kim, B., Kim, J. H. and Kim, E. (2012). Nanopatterning of Mesoporous Inorganic Oxide Films for Efficient Light Harvesting of Dye-Sensitized Solar Cells. *Angewandte Chemie International Edition*, 51(28): 6864-6869.

Kim, T., Kim, J. H., Kang, T. E., Lee, C., Kang, H., Shin, M. and Kim, B. J. (2015). Flexible, highly efficient all-polymer solar cells. *Nature communications*, 6(1): 8547.

Koleilat, G. I., Levina, L., Shukla, H., Myrskog, S. H., Hinds, S., Pattantyus-Abraham, A. G. and Sargent, E. H. (2008). Efficient, stable infrared photovoltaics based on solution-cast colloidal quantum dots. *ACS nano*, *2*(5): 833-840.

Konstantatos, G. and Sargent, E. H. (2010). Nanostructured materials for photon detection. *Nature nanotechnology*, 5(6): 391-400.

Lai, W. H., Su, Y. H., Teoh, L. G. and Hon, M. H. (2008). Commercial and natural dyes as photosensitizers for a water-based dye-sensitized solar cell loaded with gold nanoparticles. *Journal of Photochemistry and Photobiology A: Chemistry*, 195(2-3):307-313.

- Law, M., Greene, L. E., Johnson, J. C., Saykally, R. and Yang, P. (2005). Nanowire dye-sensitized solar cells. *Nature materials*, 4(6): 455-459
- Lee, H. J., Liu, Y., Coull, B. A., Schwartz, J. and Koutrakis, P. (2011). A novel calibration approach of MODIS AOD data to predict PM 2.5 concentrations. *Atmospheric Chemistry and Physics*, *11*(15):7991-8002.
- Li, G., Zhu, R. and Yang, Y. (2012). Polymer solar cells. *Nature photonics*, 6(3):153-161.
- Liu, C. Y., Holman, Z. C. and Kortshagen, U. R. (2009). Hybrid solar cells from P3HT and silicon nanocrystals. *Nano letters*, 9(1): 449-452.
- Liu, J., Wang, J., Liu, Y., Xian, K., Zhou, K., Wu, J. and Ye, L. (2023). Toward efficient hybrid solar cells comprising quantum dots and organic materials: progress, strategies, and perspectives. *Journal of Materials Chemistry A*, 11(3):1013-1038.
- Luther, J. M., Law, M., Beard, M. C., Song, Q., Reese, M. O., Ellingson, R. J. and Nozik, A. J. (2008). Schottky solar cells based on colloidal nanocrystal films. *Nano letters*, *8*(10): 3488-3492.
- Nozik, A. J. (2002). Quantum dot solar cells. *Physica E: Low-dimensional Systems and Nanostructures*, *14*(1-2): 115-120.
- O'regan, B. and Grätzel, M. (1991). A low-cost, high-efficiency solar cell based on dye-sensitized colloidal TiO2 films. *nature*, 353(6346):737-740.
- Sargent, E. (2005). Infrared quantum dots. *Advanced Materials*, 17(5): 515-522.
- Shah, A. V., Platz, R. and Keppner, H. (1995). Thin-film silicon solar cells: a review and selected trends. *Solar energy materials and solar cells*, 38(1-4):501-520.
- Sharma, S., Jain, K. K. and Sharma, A. (2015). Solar cells: in research and applications—a review. *Materials Sciences and Applications*, 6(12):1145-1155.
- Tang, H., Liang, D., Qiu, R. L. and Gao, X. P. (2011). Two-dimensional transport-induced linear magneto-resistance in topological insulator Bi2Se3 nanoribbons. *ACS nano*, 5(9): 7510-7516.
- Trihutomo, P., Marji, M., Harly, M., Wahyudi, B. A. and Radja, M. B. (2022). The effect of Clathrin protein addition

- on increasing the number of electrons in organic Dye-Sensitized Solar Cell (DSSC). *EUREKA: Physics and Engineering*, 2:15-27.
- Wang, X., Weng, Q., Yang, Y., Bando, Y. and Golberg, D. (2010). Hybrid two-dimensional materials in rechargeable battery applications and their microscopic mechanisms. *Chemical Society Reviews*, 45(15): 4042-4073.
- Wong, J. H., Royapoor, M. and Chan, C. W. (2016). Review of life cycle analyses and embodied energy requirements of single-crystalline and multi-crystalline silicon photovoltaic systems. *Renewable and sustainable energy reviews*, 58:608-618.
- Yella, A., Lee, H. W., Tsao, H. N., Yi, C., Chandiran, A. K., Nazeeruddin, M. K. and Grätzel, M. (2011). Porphyrinsensitized solar cells with cobalt (II/III)-based redox electrolyte exceed 12 percent efficiency. *science*, *334*(6056): 629-634.
- Yu, W. W., Qu, L., Guo, W. and Peng, X. (2003). Experimental determination of the extinction coefficient of CdTe, CdSe, and CdS nanocrystals. *Chemistry of materials*, 15(14): 2854-2860.
- Zhang, C., Huang, Y., Huo, Z., Chen, S. and Dai, S. (2009). Photoelectrochemical effects of guanidinium thiocyanate on dye-sensitized solar cell performance and stability. *The Journal of Physical Chemistry C*, 113(52): 21779-21783.
- Zhang, Q., Jin, T., Ye, X., Geng, D., Chen, W. and Hu, W. (2021). Organic field effect transistor-based photonic synapses: materials, devices, and applications. *Advanced Functional Materials*, 31(49):2106151.
- Zhang, Y., Kan, Y., Gao, K., Gu, M., Shi, Y., Zhang, X. and Jen, A. K. Y. (2020). Hybrid quantum dot/organic heterojunction: A route to improve open-circuit voltage in PbS colloidal quantum dot solar cells. ACS Energy Letters, 5(7): 2335-2342.
- Zhao, D. W., Liu, P., Sun, X. W., Tan, S. T., Ke, L. and Kyaw, A. K. K. (2009). An inverted organic solar cell with an ultrathin Ca electron-transporting layer and MoO3 hole-transporting layer. *Applied Physics Letters*, 95: 15
- Zhou, R., Niu, H., Ji, F., Wan, L., Mao, X., Guo, H. and Cao, G. (2016). Band-structure tailoring and surface passivation for highly efficient near-infrared responsive PbS quantum dot photovoltaics. *Journal of Power Sources*, 333: 107-117.